

Optimization of the Ion-Cut Process in Si and SiC

O. W. Holland,* D. K. Thomas,* and R. B. Gregory**

*Oak Ridge National Laboratory, Oak Ridge, TN 37831-6048

**Motorola Inc., Tempe, AZ 85284

ABSTRACT

H⁺-implantation is the basis for an ion-cut process, which combines hydrophilic wafer bonding, to produce heterostructures over a wide range of materials. This process has been successfully applied in Si to produce a commercial silicon-on-insulator material. The efficacy of implantation to produce thin-film separation was studied by investigation of H⁺-induced exfoliation in Si and SiC. Experiments were done to isolate the effects of the hydrogen chemistry from that of implant damage. Damage is manipulated independently of H⁺ dosage by a variety of techniques ranging from elevated temperature irradiation to a two-step implantation scheme in Si, and the use of channeled-ion implantation in SiC. The results will demonstrate that such schemes can significantly reduce the critical dose for exfoliation.

INTRODUCTION

The ion-cut process utilizes both hydrogen implantation and wafer bonding [1] to form thin-film heterostructures [2]. Stress generated by hydrogen implantation can cause physical separation within a solid at or near the range of the ions, R_p . Wafer bonding constrains this separation to occur laterally so that the bonded pair completely separates resulting in transfer of the superficial layer (i.e., the layer at the surface of the implanted wafer ahead of R_p). This transfer process forms the heterostructure and can be repeated using different materials to yield complex, multilayer structures. Ion-cut is presently used commercially to produce a silicon-on-insulator (SOI) heterostructure [3]. The utility of this process to produce thin-film heterostructures ultimately depends upon its economy and the quality of the transferred thin-films. Therefore, it is important to develop optimization schemes that reduce the critical hydrogen dose for affecting separation, and minimize the deleterious effects of ion-induced damage.

This paper reports the development of several schemes for optimization ion-cutting in Si and SiC. The technological importance of these materials is well known, and the ability to use them to form a heterostructure provides a tremendous tool for engineering materials. In particular, SiC is a wide band-gap semiconductor that is targeted to replace Si in high-power, high-temperature electronic applications. Ion-cutting may impact this development by making it possible to manufacture hybrid integrated circuits fabricated on a composite substrate containing both materials.

EXPERIMENTAL PROCEDURE

Irradiation was done with a raster-scanned beam of 60 keV H⁺-ions at an average current density of $\sim 2 \mu\text{amps}/\text{cm}^2$. Random implants were nominally done with the sample normal tilted 7° relative to the incident ions, while no tilt was used for channeled-ion implantation. Samples were mounted on a holder that was resistively heated to achieve the desired implantation temperature. Si(100) wafers used in this study were n-type with a resistivity of $\sim 10^{-3} \text{cm}$, while

the 4H-SiC (1000) wafers used were n-type, research grade material obtained from Cree Research with a resistivity of $\sim 0.1 \text{ } \Omega\text{-cm}$. Rutherford backscattering analysis (RBS) was done using 2.3 MeV He^{++} -ions and a solid state, surface-barrier detector positioned at 160° . Channeling spectra were acquired with the sample aligned along the major axis normal to the surface. Damage profiles were extracted from the spectra data using standard techniques.

In the absence of bonding, physical separation within an H^+ -implanted sample results in blistering/exfoliation of the superficial layer. This phenomenon derives from the same underlying mechanism as thin-film transfer and was used in this study to monitor the ion-cut process. A critical dose is defined as the minimum dose of hydrogen needed to cause blistering/exfoliation during furnace annealing in Ar at $600^\circ\text{C}/15 \text{ min}$. These blisters can be quite large (~ 10 microns diameter) and are therefore easily detected by an optical microscope. An exfoliated blister produces a crater that can be easily identified by noting the focal plane at the crater bottom to be well below the surface.

RESULTS AND DISCUSSION; PROCESS OPTIMIZATION IN Si

Implantation produces a rather inhomogeneous distribution of hydrogen around the ion range, R_p . The chemical activity and high diffusivity of hydrogen in Si cause it to quickly become bound by the ion-induced displacement damage to form a variety of defect complexes [4]. Thermal evolution leads to the formation of progressively more complex, hydrogenated defects such as the platelet [5], which plays an important role in the ion-cutting process. It consists of extended, hydrogen-terminated internal surfaces along either (100) or (111). Microcracks can occur within the platelet when trapped H_2 gas becomes pressurized at higher temperatures. This cracking expands by growth or coalescence with other microcracks up to a critical size where physical separation occurs within the lattice [6]. Figure 1 shows a simplified drawing of a platelet containing a gas inclusion. It is worth reiterating that the separation process depends upon both the unique structure of the platelet defect and the availability of hydrogen gas to provide internal pressure. Platelets are seen in the high resolution, cross-section electron micrograph (XTEM) from a Si(100) implanted with 60 keV H^+ shown in Fig. 2. Platelets are distributed with the larger defects found nearer R_p , where the hydrogen concentration is greatest. Contrast is seen within many of the defects that is clearly consistent with the existence of gas inclusions as assumed in the model.

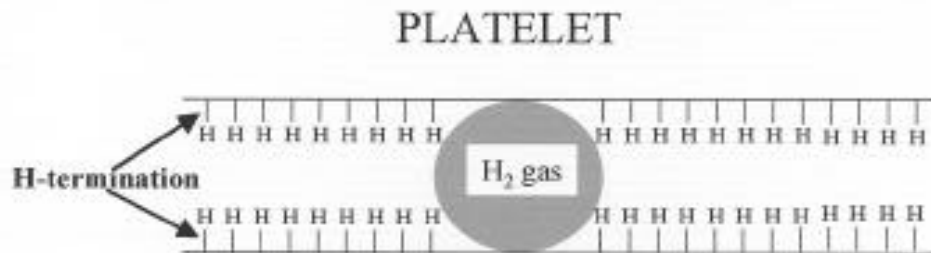


Figure 1. Drawing of platelet showing the hydrogen-terminated planar surfaces and a gas inclusion.

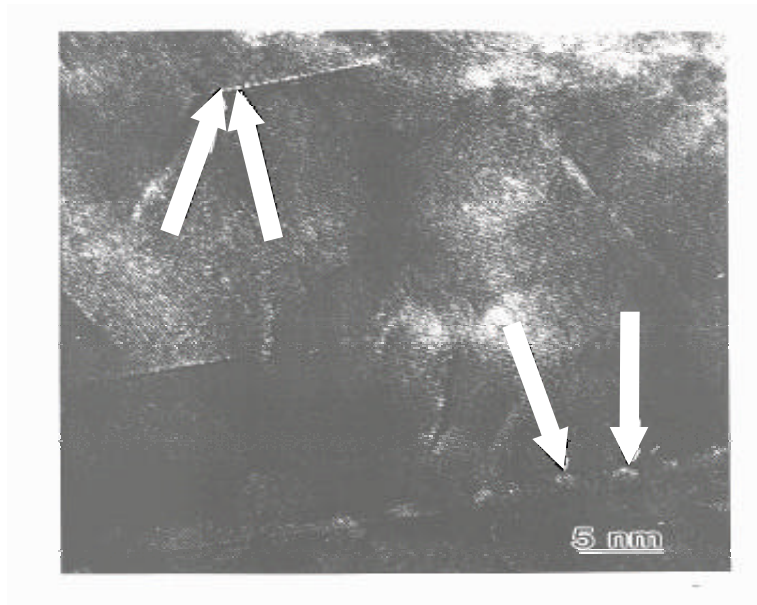


Figure 2. XTEM of Si implanted at 600°C with 60 keV H^+ -ions to a dose of $5 \times 10^{16} \text{ cm}^{-2}$. The arrows point to regions where contrast indicates an inclusion within the platelet. Note that the region at the top of the micrograph is nearer the surface while the bottom images a region near R_p .

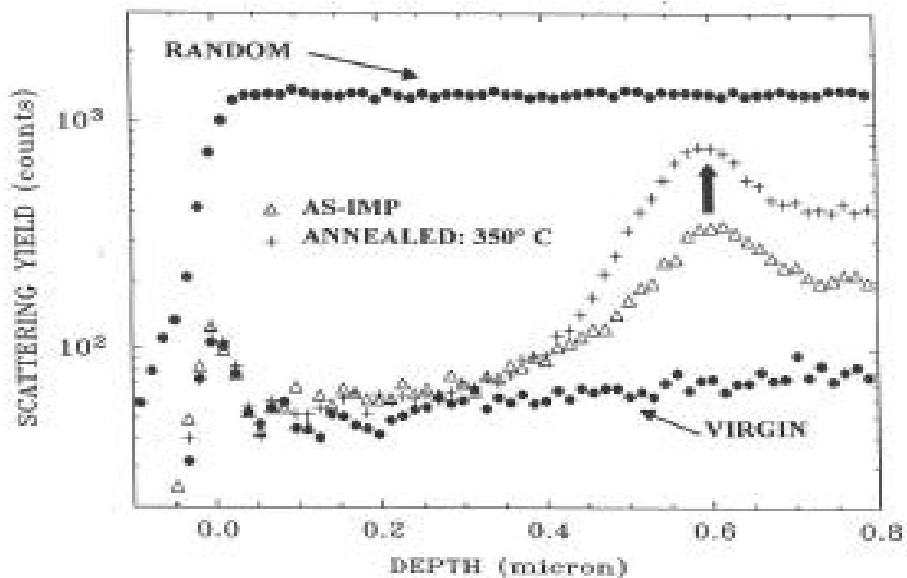


Figure 3. Comparison of aligned spectra from Si implanted at room temperature (RT) to a dose of $4 \times 10^{16} \text{ cm}^{-2}$ before and after 350°C/15 min. annealing. Random and aligned spectra from a virgin sample are shown for reference. Standard energy-loss values were used to convert the backscattering energy of the ion to a scattering depth.

Ion channeling spectrometry is typically used to characterize ion-induced damage as well as its annealing behavior. Spectra in Fig. 3 indicate that the thermal evolution of ion-induced damage in H^+ -implanted Si is complex. The scattering peak (at $\sim 0.6 \mu\text{m}$ below the surface) in the as-implanted sample is typical for most implanted samples, but the increase in the peak

height after cycling at 350°C is not. This “reverse” annealing indicates that the damage level somehow increases during thermal cycling. Since elimination or reduction of lattice damage normally minimizes the free-energy of the lattice, the apparent increase in damage seems to be thermodynamically improbable. Others have reported a similar effect and even have noted a ten-fold increase in the height of the damage peak after post-implantation annealing [7,8]. It is clear that the presence of hydrogen substantially affects the thermal evolution of the damage microstructure. This is seen in Fig. 4 where the damage or displacement field, extracted from the spectral data, is compared with TRIM simulated profiles of the implanted ions and the deposited energy. It is immediately clear that the displacement field correlates strongly with the hydrogen profile in the sample rather than the deposited energy.

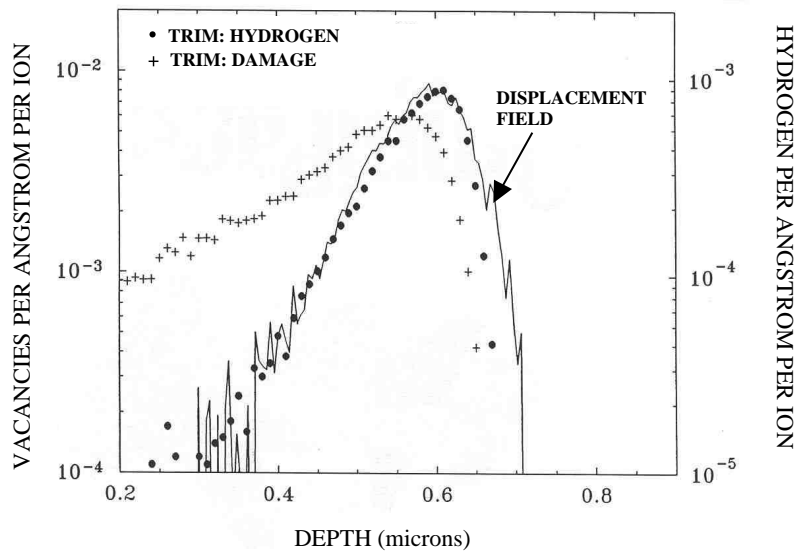


Figure 4. Comparison of the displacement field (from the annealed sample in Fig. 3) with computer-simulated profiles of the implanted hydrogen and the as-implanted defect production.

The similarity between the displacement field and the hydrogen profile suggests that this field may be monitored to gauge the hydrogen activity within the lattice. To this end, it is important to understand the specific nature of the hydrogen activity responsible for the behavior of the displacement field (e.g., the large enhancement produced by thermal cycling). The temperature range that evokes the largest response in the displacement field closely matches the range where a large fraction of the hydrogen undergoes a transition between bound and unbound states as observed by Weldon [9]. As discussed earlier, the thermal evolution of hydrogen into unbound states involves the formation of pressurized gas inclusions within platelet that cause microcracking. Cracking produces a relative displacement between regions on either side of the platelet by an arbitrarily amount (i.e., not an integral number of lattice spacings). This disrupts the registry within the lattice making it impossible for an ion beam traversing a crack to remain channeled. An ion beam aligned with the lattice on one side of the crack will, in general, be misaligned in the other. The existence of these misaligned regions (relative to the ions) can easily account for the anomalous increase in the scattering yield associated with microcracking. Based upon these arguments, it is reasonable to conclude that the thermal response of the

displacement field is due largely to microcracking, and thus is a relative measure of the efficiency of a given process to produce exfoliation.

The existence of bound and unbound states provides competing pathways for thermal evolution of hydrogen that can be manipulated to yield a more optimum process. One way to decrease the fraction of bound hydrogen is simply vary the implant temperature [10]. Dynamic annealing of the ion-induced damage provides fewer defects to trap the hydrogen. The displacement fields are compared in Fig. 5 from samples implanted at different temperatures. The peak value is greater in the 350°C implant than the RT implanted sample, even after annealing at 350°C. This suggests that a lower hydrogen dose is needed at this temperature to exfoliate the wafer (than at RT). In fact, this is the case. Elevated temperature implanted yield a critical dose of $3.5 \times 10^{16} \text{cm}^{-2}$ compared to $4.1 \times 10^{16} \text{cm}^{-2}$ at RT. Next, it is seen that the displacement field is shifted towards the surface in the sample irradiated at high temperature. The shift moves the field closer to the peak of the damage profile, as shown in Fig. 4. Since dynamic annealing at the higher temperature eliminates much of the ion-induced damage, there appears to be an insufficient amount to completely trap the hydrogen at the R_p location. Hydrogen therefore diffuses within the lattice until it finds the damage at the peak of the deposited energy profile. There the hydrogen is trapped and can participate in the ion-cut process. This is a case of “undertrapping” where insufficient residual damage is present at R_p to completely trap the implanted hydrogen. Some of the diffusing hydrogen obviously avoids being trapped and is lost to the bulk. Conversely, hydrogen implanted at RT is clearly “overtrapped.” Too much of the hydrogen becomes trapped such that an insufficient amount is available as hydrogen gas to pressurize the defects. The temperature that yields an optimal balance between the competing pathways must lie between these values.

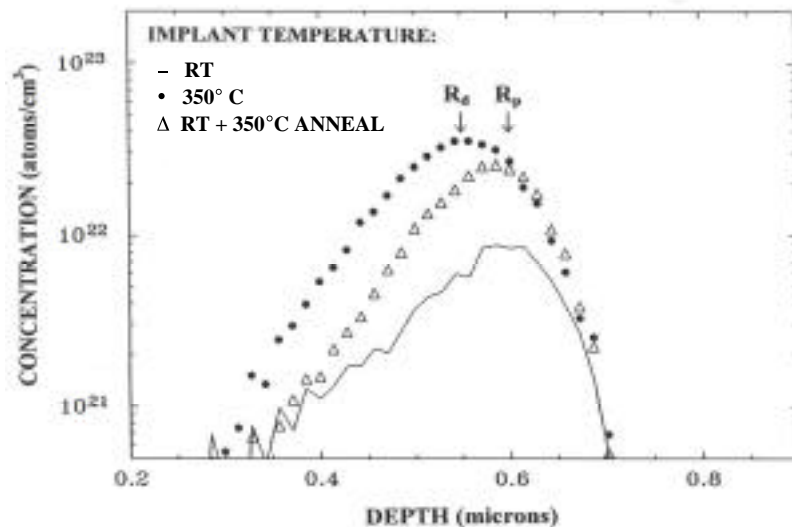


Figure 5. Comparison of the displacement field in Si after implantation at RT and 350°C to a dose of $4 \times 10^{16} \text{cm}^{-2}$. The displacement field after 350°C annealing of the RT implanted sample is also shown. The comparison yields two observations: (1) the field in the RT sample remains peaked near R_p even after annealing and (2) the field after implanting at 350°C is located near the damage peak as shown in Fig. 4.

It should be noted that, despite its benefits, there are some potential problems with high temperature irradiation. Spectra in Fig. 6 compare the aligned yield from samples implanted at different temperatures after annealing at 450°C. The scattering yield is greater, especially from the superficial region, in the sample implanted at high temperature indicating a higher level of damage than in the RT implanted sample. As discussed above, irradiation at high temperature may result in an undertrapped condition where there the damage near R_p is insufficient to immobilize all the hydrogen. In such a case, a portion of the hydrogen is available to diffuse widely within the lattice. Hydrogen appears to have diffused into the superficial region and formed stable hydrogenated defect complexes. This clearly raises a concern about the quality of the material within this region. Since the superficial region is transferred during ion-cutting, its quality is of paramount importance. Electrical measurements are needed to determine the effects of this residual damage.

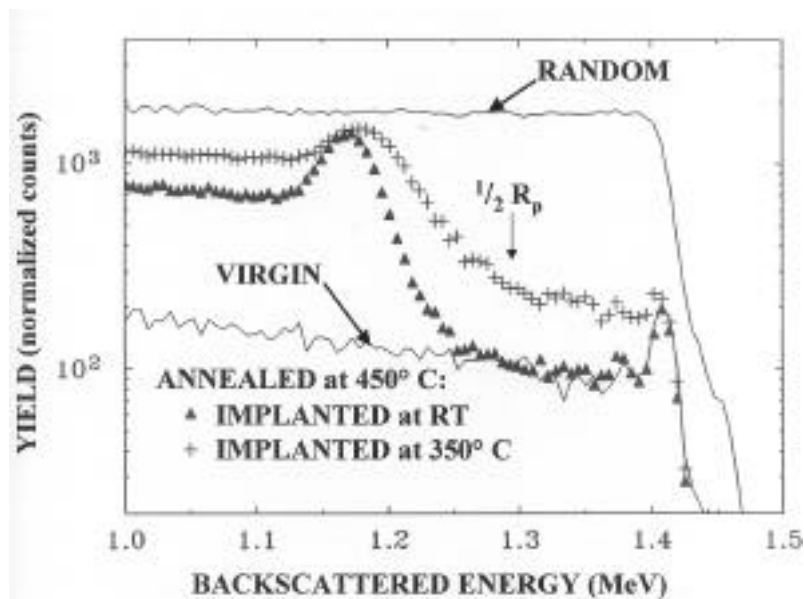


Figure 6. Aligned spectra comparing the effect of implantation temperature (i.e., RT and 350°C) on the quality of the superficial layer after 450°C/15 min. furnace annealing. Both samples were implanted with a dose of $4 \times 10^{16} \text{ cm}^{-2}$. There is little or no damage in the RT implanted sample to a depth of $\sim R_p$ while damage extends to the surface in the sample implanted at 350°C. Random and aligned spectra from virgin Si are shown for reference

Means of reducing the critical dose without resorting to elevated temperature irradiation were explored. This is important because the expense and time incurred doing such implants more than cancel any benefit. Thus, an attempt was made to manipulate the various pathways for implanted hydrogen by static rather than dynamic means. This was done using a two-step, RT irradiation process in which the implantation is interrupted to ex-situ treat the samples. The details are as follows. A portion of the total dose is initially implanted that is sufficient to form a distribution of platelet defects near the ion range. The sample is then removed from the implanter and annealed at 350°C in a standard furnace in an Ar ambient. It is reasonable to assume that this anneal promotes both nucleation and growth of the platelets. This procedure profoundly affects the behavior of hydrogen subsequently implanted. This is seen in Fig. 7

where the critical dose for two-step processing is shown to be much smaller than that achieved by standard processing. In the figure, the critical dose is expressed as a function of various two-step processes. Although the critical dose is fairly insensitive to the initial dose (over the range studied), a minimum value of $2.75 \times 10^{16} \text{cm}^{-2}$ was found, a 33% reduction over single-step processing at RT. It is not completely clear why two-step processing yields such a marked reduction in the critical dose. However, the thermally ripened platelets may be more efficient in getting the subsequently implanted hydrogen. This would tend to suppress the formation of new platelets making even more hydrogen available to pressurize the defects.

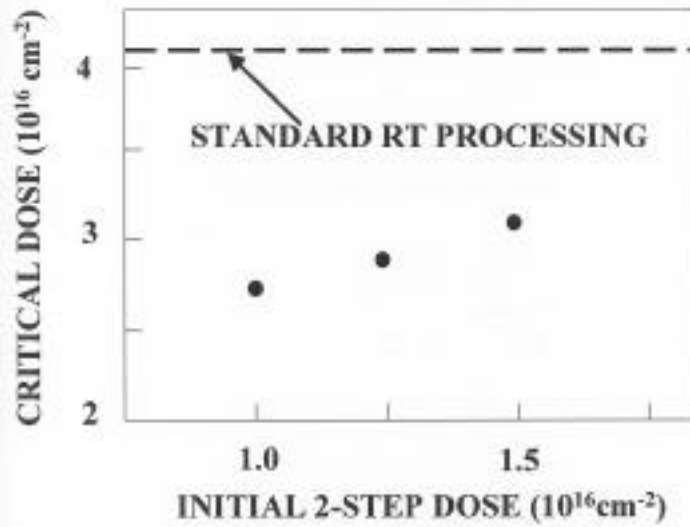


Figure 7. A plot of the critical dose for various two-step processes indicated by the dose of the initial implant step. The critical dose for a standard, single-step process is indicated by the dashed line.

RESULTS AND DISCUSSION; PROCESS OPTIMIZATION IN SiC

Silicon carbide, SiC, offers a unique challenge to the ion-cut process. In particular, it has been shown that light ion irradiation of single-crystal SiC material results in substantial deactivation of as-grown dopants that does not recover even after annealing at 1200°C [11]. Therefore, it was not surprising when thin-films cut from low resistivity material by hydrogen implantation were found to be highly resistive, and thus useless for electronic applications [12]. Any optimization process in SiC must address this issue of dopant deactivation. While decreasing the critical dose may help (by reducing the total amount of ion-induced damage), a more specific technique is needed to selectively target the damage in the superficial region. Fortunately, channeled-ion implantation is such a technique. Channeling is accomplished by aligning a single crystal along a major crystallographic direction with the incident ions so that the motion of the ions is constrained to the channels or interstices of the lattice [13]. As such, the ions interact weakly with the lattice atoms especially in the near-surface ahead of R_p so that the occurrence of displacements events is greatly reduced. Figure 8 compares aligned spectra from SiC samples implanted with hydrogen (60 keV, $2.5 \times 10^{16} \text{cm}^{-2}$, RT) along random and

channeled directions. The relative scattering yield in the spectra indicates that channeled-ion implantation is much more successful (than random) in suppressing damage formation, especially in the region ahead of $1/2 R_p$.

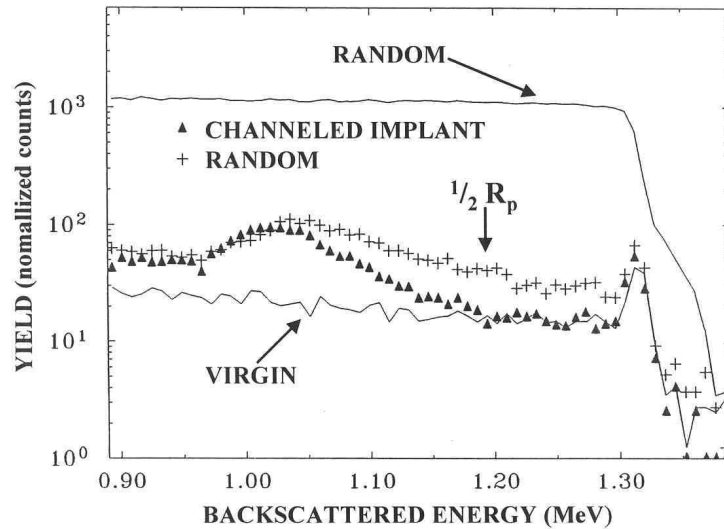


Figure 8. Comparison of aligned spectrum from Si implanted either along a random direction or channeled along a $[1000]$ axis. The irradiation was done at RT with a dose of $2.5 \times 10^{16} \text{ cm}^{-2}$.

A collateral effect was observed for channeled-ion implantation that may be anticipated from a closer examination of the spectra in Fig. 8. These spectra show that the scattering yield for the channeling implant is lower than random over the entire range. The lower damage level near R_p suggests that channeled-ion implantation may have an effect upon the critical dose [14]. As discussed earlier, various pathways exist for the hydrogen during thermal evolution. In the case of overtrapping, too much of the hydrogen is bound by the damage so that insufficient amounts are available to form hydrogen gas. In such a case, the critical dose will be reduced by any implant technique that lowers damage levels (near R_p). This, in fact, is exactly what occurs for channeled-ion implants in SiC. The critical dose was determined to be $3.25 \times 10^{16} \text{ cm}^{-2}$ for a channeled implant compared to $4.5 \times 10^{16} \text{ cm}^{-2}$ for random. Similar effects have been observed in Si but will be reported elsewhere.

A summary of the results comparing damage levels for channeled and random implants are shown in Fig. 9 for a wide range of ion dose. Arrows in the figure indicate the critical dose for both implants. It is clear that channeling results in a substantial reduction in the yield at $1/2 R_p$ over the entire dose range. However, no damage (i.e., deviation from the virgin level) was measured at the channeling critical dose. Thus, channeled-ion implantation is able to introduce a critical dose of hydrogen into the SiC lattice without causing measurable damage to the superficial layer. A four-point resistivity measurement was done to determine the state of the superficial layer after implantation. A subcritical dose of $2 \times 10^{16} \text{ cm}^{-2}$ was used since annealing at 1200°C was done prior to the measurement. This was necessary since exfoliation at higher doses makes it impossible to test the sample. A value for the resistivity was obtained for the channeled implant but not the random, which was too high to measure. However, the measured resistivity for the channeled implant was lower than anticipated and, probably, did not accurately

reflect the property of the superficial layer. Initially, the residual damage at R_p was considered to be sufficient to electrically isolate the superficial layer from the bulk during testing, but the lower value may reflect that this was not the case. Clearly more electrical testing needs to be done to ascertain the effects of channeled-ion irradiation but this preliminary result is encouraging.

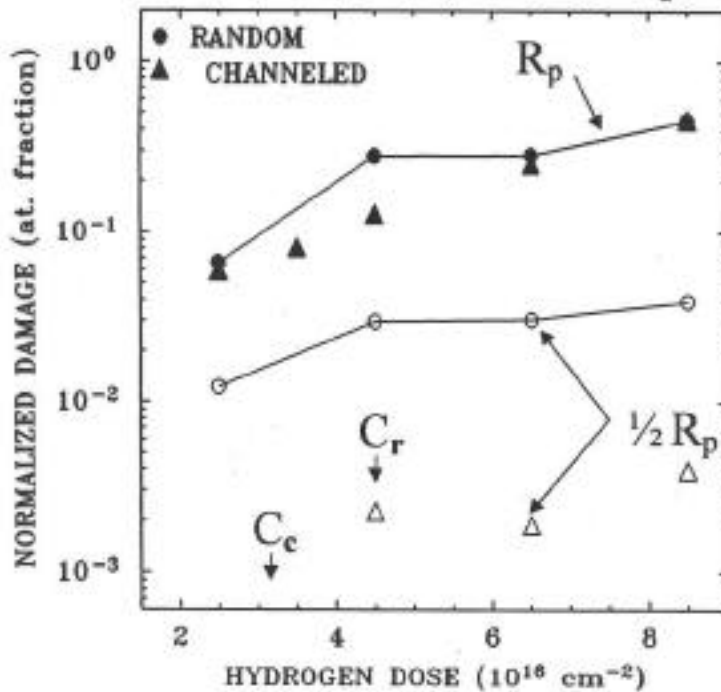


Figure 9. Normalized damage at depths, R_p and $\frac{1}{2}R_p$, versus hydrogen dose for RT channeled and random implants in SiC. The critical dose for channeled and random implants is indicated by arrows marked as C_c and C_r , respectively.

CONCLUSIONS

Optimization of the implantation conditions to effect physical separation within either Si or SiC was discussed. A variety of techniques from elevated temperature irradiation to a two-step implantation scheme were demonstrated to be effective in Si for lowering the critical dose, while channeled-ion implantation of SiC was shown to both lower the critical dose and yield a transfer layer of higher quality. A physical basis to understand these effects was discussed and related to the microscopic behavior of hydrogen within the crystal lattice. Clearly, further optimization could be achieved by a judicious combination the various techniques.

ACKNOWLEDGEMENTS

The authors would like to acknowledge D. Fathy for XTEM analysis of the implanted samples. Oak Ridge National Laboratory, managed by UT-Battelle, LLC, for the U.S. Dept. of Energy under contract DE-AC05-00OR22725.

REFERENCES

1. Q.-Y. Tong and U. Gössele, *Semiconductor Wafer Bonding: Science and Technology*, John Wiley & Sons, Inc., New York, 1999.
2. M. Bruel, "Process for the production of thin semiconductor material films," *US patent* 5,374,564 (1994).
3. M. Bruel, *Electron. Lett.*, **31**, 1201 (1995).
4. G. F. Cerofoline, R. Balboni, D. Bisero, F. Corni, S. Frabboni, G. Ottaviani, R. Tonini, R. S. Brusa, A. Zecca, M. Ceschini, G. Giebel, and L. Pavesi, *Phys. Stat. Sol. (a)*, **150**, 539 (1995).
5. J. N. Heyman, J. W. Ager III, E. E. Haller, N. M. Johnson, J. Walker, and C. M. Doland, *Phys. Rev. B*, **45**, 13363 (1992).
6. L.-J. Huang, Q.-Y. Tong, Y.-L. Chao, T.-H. Lee, T. Martini, and U. Gössele, *Appl. Phys. Lett.*, **74**, 982 (1999).
7. J. Keinonen, M. Hautala, E. Rauhala, V. Karttunen, A. Kuronen, J. Räisänen, J. Lahtinen, A. Vehanen, E. Punkka, and P. Hautojärvi, *Phys. Rev. B*, **37**, 8269 (1988).
8. B. Bisero, F. Corni, S. Frabboni, R. Tonini, and G. Ottaviani, *J. Appl. Phys.*, **83**, 4106 (1998).
9. M. K. Weldon, M. Collot, J. Chabal, V. C. Venezia, A. Agarwal, T. E. Haynes, D. J. Eaglesham, S. B. Christman, and E. E. Chaban, *Appl. Phys. Lett.*, **73**, 3721 (1998).
10. R. B. Gregory, T. A. Wetteroth, S. R. Wilson, O. W. Holland, and D. K. Thomas, *Appl. Phys. Lett.*, **75** (1999).
11. M. K. Linnarsson, M. Janson, A. Schöner, N. Nordell, S. Karlsson, and B. G. Svensson, *Mater. Sci. Forum*, **264-268**, 761 (1998).
12. Unpublished results.
13. See for example, Wei-Kan Chu, James W. Mayer, and Marc-A. Nicolet, *Backscattering Spectrometry*, Academic Press, New York, (1978) p. 223.
13. R. B. Gregory, O. W. Holland, D. K. Thomas, T. A. Wetteroth, and S. R. Wilson, *Mat. Res. Soc. Symp. Proc.*, **572**, 33 (1999).